Recueil De Mécanique
Centre Universitaire
El Wancharissi de Tissemsilt

Research Paper *DOI : 10.5281/zenodo.2581404* *Open access*

Predictive diagnosis of unbalance and misalignment defects Based on the FFT and DWT of the stator current of an induction motor: Experimental approaches

Diagnostic prédictif de défauts de balourd et de mésalignement basé sur la FFT et la DWT du courant statorique d'un moteur à induction : Approches expérimentales

Chemes Eddine ROUABHIA [a,*], ***Slimane BOURAS*** [b], ***Abdelkarim BOURAS*** [c]

[a] *Electromechanical Engineering Laboratory, Department of Electromechanical, Badji Mokhtar University, B.P.12, 23000, Annaba , Algeria.*

[b] *The industrial risks, C.N.D, S.O.M.M laboratory, Department of Electromechanical, Badji Mokhtar University, B.P.12,23000, Annaba , Algeria.*

[c] *Electromechanical Systems Laboratory, Department of Electromechanical, Badji Mokhtar University, B.P.12,23000, Annaba, Algeria.*

ARTICLE INFO

Article history :

Received 15 October 18

Received in revised form 11 January 19

Accepted 24 January 19

Keywords:

Asynchrnous motor; Mechanical faults; Wavelet transform; FFT of Park vector

Mots clés:

Moteurs asynchrones; défauts mécaniques; Transformée en ondelettes; FFT du vecteur de Park

ABSTRACT

Because of the complexity of their modelling, mass imbalance and engine misalignment have not received much attention from researchers. Early, correct and reliable detection of these defects helps to stop the propagation of the failure or limits its evolution to severe degrees. Thus, the purpose of this paper is to extract the frequency signatures of the unbalance and misalignment in the stator current signal from the start of the induction motor using the Fast Fourier Transform (FFT) of the Park current vector supplemented by the Discrete Wavelet Transform (DWT). The experimental validation carried out on a 2.6 Kw "Leroy Somer" induction motor gave satisfactory results that can be operated by trained maintenance personnel who are not necessarily highly qualified in the field.

RÉSUMÉ

En raison de la complexité de leur modélisation, le déséquilibre de masse et le désalignement du moteur n'ont pas fait l'objet d'une grande attention de la part des chercheurs. Une détection précoce, correcte et fiable de ces défauts permet d'arrêter la propagation de la défaillance ou de limiter son évolution à des degrés sévères. Ainsi, le but de cet article est d'extraire les signatures de fréquence du balourd et du désalignement dans le signal du courant statorique dès le démarrage du moteur en utilisant la transformée de Fourier rapide (FFT) du vecteur de courant de Park complétée par la Transformée d'Ondelettes Discrètes (DWT). La validation expérimentale effectuée sur un moteur à induction "Leroy Somer" de 2,6 Kw a donné des résultats satisfaisants qui peuvent être utilisés par un personnel de maintenance formé et pas nécessairement hautement qualifié dans le domaine.

* *Corresponding author. Tel.: +213 671912701.*
E-mail address: sshamss2728@gmail.com

1 Introduction

Despite their robustness, asynchronous drives especially those based on high power motors, are much more often subject to mechanical failures than electrical ones [1]. Due to the improved manufacturing conditions of induction motors, electrical faults in the stator and rotor are becoming less frequent. In recent decades, the cause of the majority of degradations of rotating machines in an industrial environment is due to the defects of unbalance and misalignment.

The mass unbalance and misalignment increase the coupling reaction forces transmitted to the shaft and thus to the machine components (bearings, seals, shafts and couplings) [2,3,4,5,6]. In the presence of these mechanical defects, strong alterations of the shafts and foundation screws accompanied by a large pumping of the motor supply current are noted. In the presence of these two defects, the coupling reaction forces transmitted to the shaft and induction motor components (bearings, joints, couplings and fixing bolts) increase. A large pumping of the stator current accompanied by torque oscillation peaks very critical for the motor and the components coupled to it are observed, the cost of maintenance will be exorbitant, if these possible degradations are not detected as soon as they appear.

Traditionally, vibration signals are used to detect mechanical damage and monitor the health of rotating machines in operation. Vibration analysis through the Fast Fourier Transform (FFT) is the most recommended for the diagnosis of mechanical failures internal or external to the motor unit [7,8,9,10]. However, there are defects inducing torque fluctuations for which vibration analysis shows its limits. The high sensitivity of the electric current to the torque variations picked up by the asynchronous motor and, consequently, to the mechanical faults inducing them, makes the current analysis an extremely powerful complementary investigative tool [11,12,13]. Nevertheless, it should be noted that the detection and diagnosis of unbalance fault and misalignment through the MCSA (Motor Current Signature Analysis) did not generate much resonance among researchers, compared to electrical defects (short circuit of turns, breaking of bars, unbalance of voltages) [14,15,16,17] and the eccentricity of the gap [18,19,20,21] in the induction motor.

In order to extract precisely the information relating to these mechanical defects, some research work [22, 23] has been oriented towards the spectral analysis of the electric current through the MCSA. In this paper, we propose a diagnostic methodology and detection of unbalance and misalignment defects using the FFT of current Park vector and the Discrete Wavelet Transform (DWT). The spectrum approach through the FFT component (i_d, i_q) of the Park vector gives a more significant spectrum than the obtained by spectrum analysis (FFT) of the conventional induction motor and it saves a compact representation of the spectra of three stator currents (i_a, i_b, i_c) [24, 25,26]. However, only this technical FFT may have limitations because some elements of the system can be coupled in the spectrum, and their frequency components will be hidden, so it will be difficult to isolate the various defects. Also, in time-frequency analysis of a signal, conventional Fourier transform analysis is inadequate because the Fourier transform of a signal contains no local information. This is the major disadvantage of the Fourier transform.

This experimental work discusses the performances of the Fourier transform technique (FFT) accompanied by the DWT, these methods are applied to the stator current appear to be useful for detecting the mechanical defects mentioned above [27–29].

The relative energy for each detail tells us about the evolution and the gravity of the two aforementioned mechanical failures. Benchmarking of these two techniques gave satisfactory results. The results obtained for the healthy state will serve as a reference for future situations.

2 Material and methods

2.1 Component of Park vector current stator

Park's vector method is a simple way to see if the machine is healthy or not. It means that the phase currents (i_a, i_b, i_c) are to be transformed into a two-coordinate system with perpendicular axes (i_d, i_q) and placed on d-axis and q-axis respectively. The current park vector components are functions of main phase variables, which are expressed as:

$$i_d = \sqrt{\frac{2}{3}}\, i_a - \frac{1}{\sqrt{6}}\, i_b - \frac{1}{\sqrt{6}}\, i_c \tag{1}$$

$$i_q = -\frac{1}{\sqrt{2}} i_b - \frac{1}{\sqrt{2}} i_c \tag{2}$$

2.2 Fourier frequency analysis

In order to characterize the origin of the defects, many signal processing tools are used [30, 31]. Among these tools the Fourier transform is well suited to analyze stationary phenomena. The component at the frequency f of a time signal x(t) is expressed by:

$$X(f) = \int_{-\infty}^{+\infty} X(f).e^{-j.2.\pi.f.t}\, dt \tag{3}$$

The mechanical defects are detected by the monitoring of the suitable frequencies of the Vibrator signal which can characterized by : [32]

$$f_{def} = n\, f_o \text{ where } n = 1,2,3,4,... \tag{4}$$

In figure (1), expressed in acceleration (g), the vibration image (fig. 1a) of the unbalance defect consists of a component that predominates at the rotation frequency of shaft f_o. On the other side, misalignment fault is revealed by the presence of a line of predominant amplitude whose frequency generally corresponds to order 2 of the rotation frequency of shaft f_o .

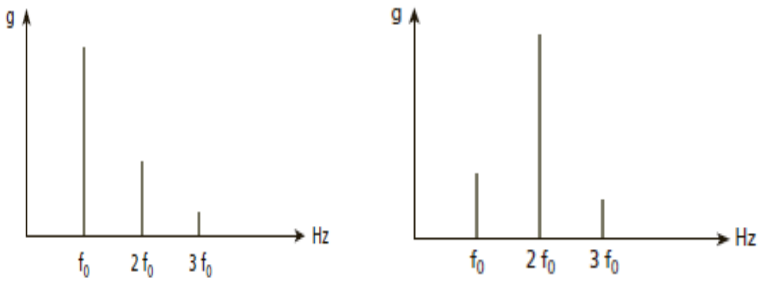

(a) (b)

Fig. 1 –Image theoretical vibration of unbalance (a) (n = 1) and misalignment (b) (n = 2) faults.

These two mechanical defects also are detected by the monitoring of the suitable frequencies of the phase of the stator current; generally, the frequency of the unbalance and misalignment faults studied in this paper is given by equation (5).

$$f_{def} = f \pm n\, f_r \tag{5}$$

Where:

- f_{def} : is the frequency of mechanical defects
- f : is the frequency of power supply with f = 50 Hz
- f_r : is the rotational frequency with n = 1, 2, 3, 4 ...

Previously, the characteristic frequency of mechanical unbalance based on current signature analysis is used as a non-invasive method to detect side band harmonics around the fundamental frequency, it is expressed by:

$$f_{unb} = f \pm 1\, f_r \tag{6}$$

Two kinds of misalignment are to be considered, angular misalignment and axial or parallel misalignment and of course a combination of the two, which constitutes the majority of misalignments, the latter generates modulated additive amplitudes and frequencies in the stator currents (Figure 1). The misalignment is a defect that will act on the shaft symmetrically twice every turn, whether it is due to a lack of concentricity, angular misalignment or shaft bending.

$$f_{mis} = f \pm 2 f_r \tag{7}$$

To diagnose mechanical unbalance and misalignment defects in an electric motor, this latter information has the ideal frequency location for a discrete wavelet transform that has already been applied directly to the stator current.

2.3 Principle of discrete wavelet decomposition

The wavelet transform divides the original signal into a time scale space, where the size of the windows at time and scale is not rigid. In our field, the wavelet transform has been used to extract the dominant characteristics of the original signals for fault diagnosis and is well suited for non-stationary signals.

The multi-resolution wavelet analysis consists of disintegrating a signal into a series of minor waves belonging to a family of wavelets, the latter being a practical version of the discrete wavelet transform. A signal f(t) could be decomposed as:

$$f(t) = \sum_{n=0}^{N} A_{m0,n} \varphi_{m0,n}(t) + \sum_{m=m0}^{m-1} \sum_{n=0}^{N} D_{m,n} \psi_{m,n}(t) \tag{8}$$

Where: $\emptyset_{m0,n}$ is the scaling function at a scale of 2^{m0} shifted by n, $\psi_{m,n}(t)$ is the wavelet function. They are expressed respectively by:

$$\varphi_{m0,n}(t) = 2^{m0/2} \varphi\left(2^{m0} t - n\right) \tag{9}$$

$$\psi_{m,n}(t) = 2^{m/2} \psi\left(2^{m} t - n\right) \tag{10}$$

That is, $\psi_{m,n}$ is the mother wavelet at a scale of 2^m shifted by n.

Generally, approximate coefficients $A_{m0,n}$ are obtained through the inner product of the original signal and the scaling function**.**

$$A_{m0,n} = \int_{-\infty}^{+\infty} f(t) \varphi_{m0,n}(t) dt \tag{11}$$

The approximate coefficients decomposed from a discretized signal can be expressed as:

$$A_{(m+1),n} = \sum_{n=0}^{N} A_{m,n} \int \varphi_{m,n}(t) . \varphi_{m+1,n}(t) dt = \sum_{n=0}^{N} A_{m,n} . g(n) \tag{12}$$

The filter g(n) is a low-pass filter. Similarly, the detail coefficients $D_{m,n}$ can be generally obtained through the inner product of the signal and the complex conjugate of the wavelet function:

$$D_{m,n} = \int_{-\infty}^{+\infty} f(t) . \psi^{*}_{m,n}(t) dt \tag{13}$$

The detail coefficients decomposed from a discretized signal can be expressed as:

$$D_{(m+1),n} = \sum_{n=0}^{N} A_{m,n} \int \varphi_{m,n}(t) . \psi_{m+1,n}(t) dt = \sum_{n=0}^{N} A_{m,n} . h(n) \tag{14}$$

In the dyadic approach, $D_{m,n}$ are the detail coefficients at a scale of 2^{m0}. The filter h(n) is a high-pass filter. The approximations and details can be determined using low and high-pass filters. In the multi-resolution analysis, the approximations are split successively, while the details are never analyzed further [33,34,35].

2.4 Energy of decomposition in wavelets

A very efficient diagnostic tool consists of calculating the energy associated with each level or each decomposition node, since the degraded state of the system is clearly distinguished from the healthy state following the relative energy associated with each level of energy decomposition so the eigenvalue of each frequency band is defined by:

$$E_j = \sum_{k=1}^{k=n} \left| E_{j,k(n)} \right|^2 \tag{15}$$

Where j : is the level of decomposition. Based on the eigenvalue of energy, the eigenvector is given by:

$$T = \left[\frac{E_0}{E}, \frac{E_1}{E}, \frac{E_2}{E}, \ldots, \frac{E_{2^m-1}}{E} \right] \tag{16}$$

With:

$$E = \sum_{j=0}^{2^m-1} \left| E_j \right|^2 \tag{17}$$

The plot of the eigenvector T which contains the current signal information in the motor is used to diagnose mechanical damage to the system through the generator current. The difference between the shape of the energy of the healthy and failing states also contributes to the identification of the degree of defect [36].

2.5 Experimental setup

Our test bench is composed of an asynchronous cage motor coupled with a DC generator; the parameters of the machines are presented in Table 1.

Table 1 - Parameters of the machines

Asynchronous cage motor (Leroy Somer)				
2.6 Kw	1450 rpm	380 V	6.9 A	50 Hz
DC Generator (Leroy Somer)				
3 Kw		220 V		14 A

The necessary material for data measurement and acquisition as well as their interpretation is composed of an ampere metric grip PAC12 and a numerical oscilloscope and a computer. At the beginning, an unbalance is generated with the fixing of a mass of 50 g on the shaft end of the engine (side coupling); then the aggregate is subjected misalignment. The misalignment of the engine with the generator is obtained by the insertion of two aluminum plates of 2 mm of thickness under the two legs before the engine. The acquisition of the three currents was made by a digital oscilloscope HAMEG507 equipped with software SP107E. The data processing is carried out using MATLAB software for signal analysis. For the acquisition of the stator current signals taken during the tests, a sampling frequency of $f_s = 1$ KHz was used for 2046 points.

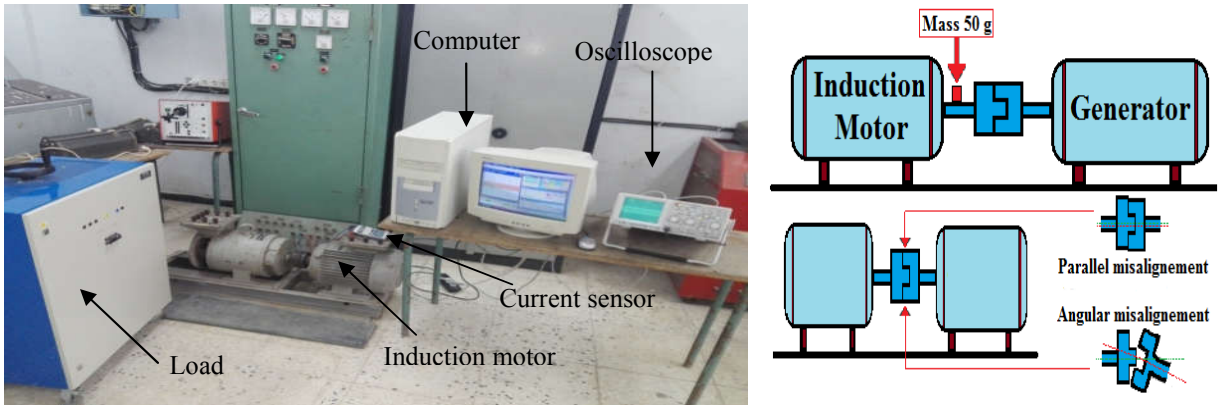

Fig. 2 – a) Test bench on aggregate of machines Leroy Somer, b) Experimental workflow

3 Results and discussion

After the starting up of the test bench presented above, it was possible to capture the stator current of the three phases which will be treated under Matlab. Figure 3 shows temporal characteristic of the captured phase electric current (case of healthy motor at no load).

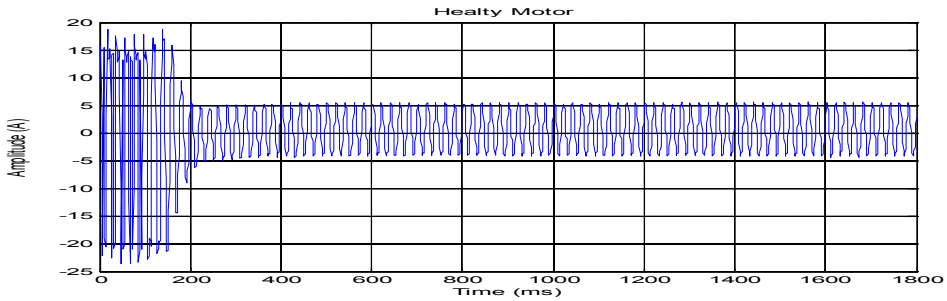

Fig. 3 – Temporal healthy current motor

3.1 Unbalance detection using FFT Park vector

Figure 4 shows the Fourier transform of the Components (i_d, i_q) in healthy and degraded case, the stator current in case of unbalance fault. The tests were conducted off load for a measured motor speed n_0 = 1485 rpm, the frequency of rotation of the motor at no load is then f_r = 24.75 Hz. The characteristic frequencies of the peaks signifying the mass unbalance are: $f_{unb} = f \pm 1.f_r = 50 \pm 24.75$ Hz. The sidebands harmonics around the fundamental supply frequency: $f_{unb} = [74.75 \text{ Hz and } 25.25 \text{ Hz}]$

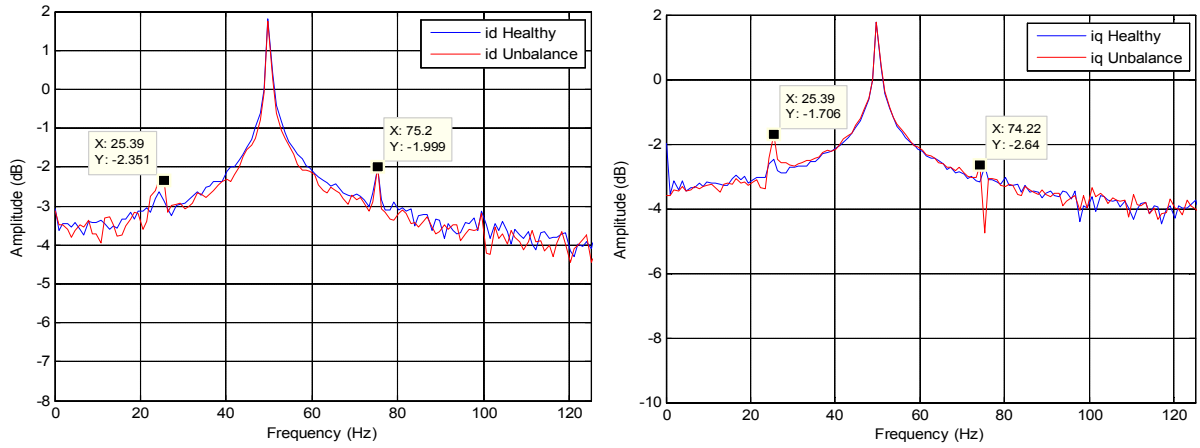

Fig. 4 – Spectrums of (i_d, i_q) component: Healthy and degraded (Unbalance) case.

3.2 Misalignment detection using FFT Park vector

Figure 5 shows the spectrum of the Park vector components $(\boldsymbol{i_d, i_q})$ of the stator current when the motor is affected by a misalignment fault. The sidebands harmonics around the fundamental supply frequency: $\boldsymbol{f_{mis} = f \pm 2.f_r = 50 \pm 49.50 \text{ Hz}}$ $\boldsymbol{\Rightarrow f_{mis} = [99.50 \text{ Hz and } 0.50 \text{ Hz}]}$. The fault frequency is clearly mentioned in the figure below which can confirm the motor defect.

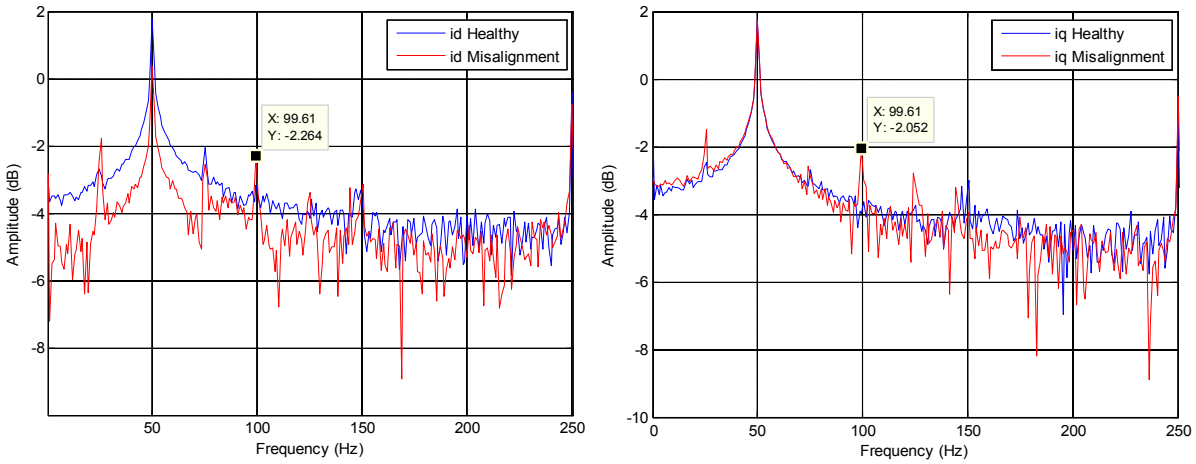

Fig. 5 – Spectrums of (i_d, i_q) component: Healthy and degraded (Misalignment) case.

3.3 Diagnosis using the discrete wavelet

Using Equation (18) and Equation (19) to calculate the required decomposition level, this multi-level decomposition of the stator current is performed using the mother wavelet 'Daubechies'.

$$n_{Ls} = \text{int}\left(\frac{\log\left(f_s/f\right)}{\log\left(2\right)}\right) \tag{18}$$

Where:

- ✓ f is the network frequency.
- ✓ f_s is the sampling frequency.

Knowing $f = 50$ Hz and $f_s = 1$ KHz, we can calculate the number of appropriate decompositions:

$$n_{Ls} + 2 = \text{int}\left(\frac{\log\left(10^3/50\right)}{\log\left(2\right)}\right) \tag{19}$$

If f_s(samples/s) is the sampling frequency for capturing the electric currents i_a, i_b and i_c, detail D_j includes information about the signal components whose frequencies are covered by the interval $[2^{-(j+1)}, 2^{-j}f_s]$. The approximation signal a_n contains the low-frequency components of the signal, which belong to the frequency interval $[0, 2^{-(n+1)}f_s]$.

Table 2 represents the different frequency bands obtained by the discrete wavelet decomposition corresponding to the high order wavelet signals resulting from the analysis, according to the sampling rate ($f_s = 1000$ Hz) used for the tests.

Table 2 - Frequency bands of detail and approximation signals

Levels	Approximations		Details	
J=1	A1	0 – 500	D1	500 – 1000
J=2	A2	0 – 250	D2	250 – 500
J=3	A3	0 – 125	D3	125 – 250
J=4	A4	0 – 62.5	D4	62.5 – 125
J=5	A5	0 – 31.25	D5	31.25 – 62.5
J=6	A6	0 – 15.625	D6	15.625 – 31.25

For the purpose of covering unbalance and misalignment defects, we have realized an acquisition system that allows raising the different signals. In this part, the DWT is applied to the signals of the stator current supplied by the Leroy Somer machine for the validation of the wavelet technique by experimental signals.

The Daubechies wavelet of order 40 (db40) was selected as mother wavelet in our multilevel decomposition of the rotor current. In order to make a comparison, in Figure 6 the approximation signals A6 are represented, the detail signals (D1 - D6) will be represented for the healthy (Figure 7) and degraded operating states in Figure 8 and Figure 9 respectively.

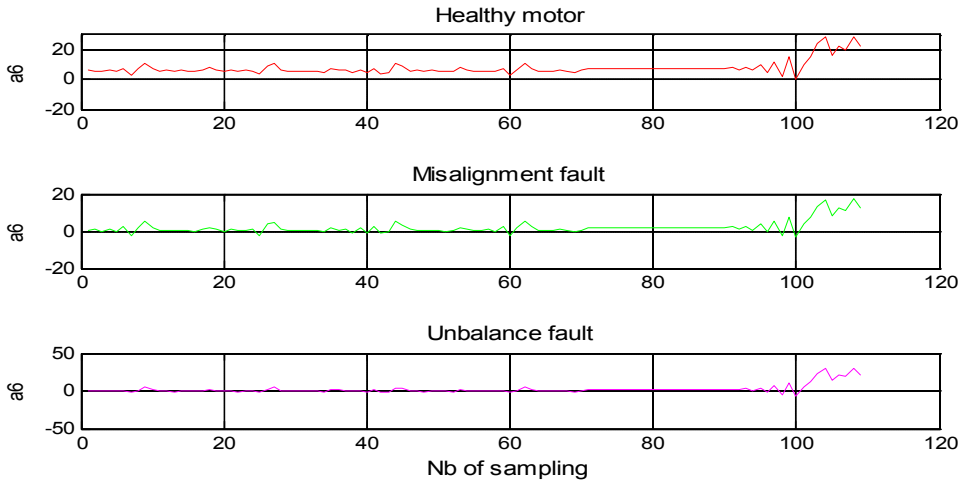

Fig. 6 – Approximation signals.

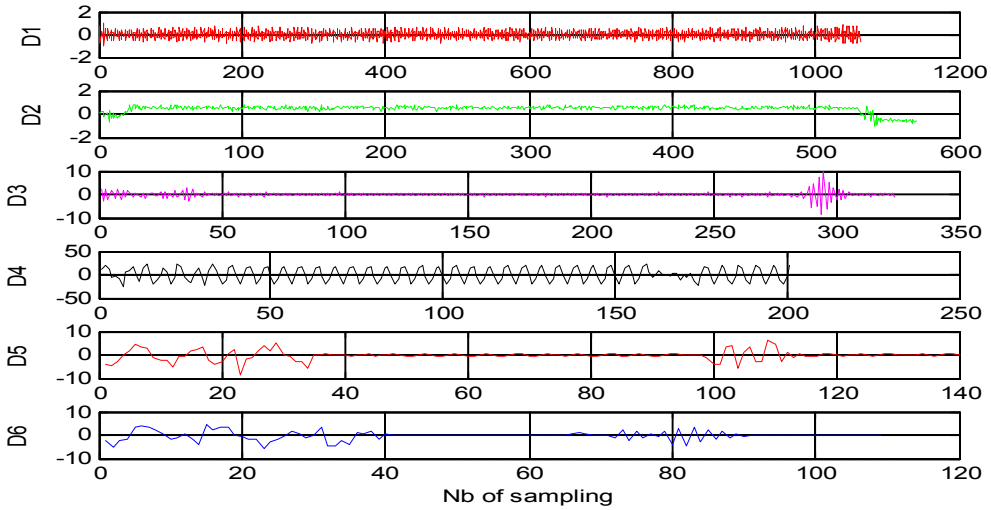

Fig. 7 – DWT of the stator current: Healthy motor.

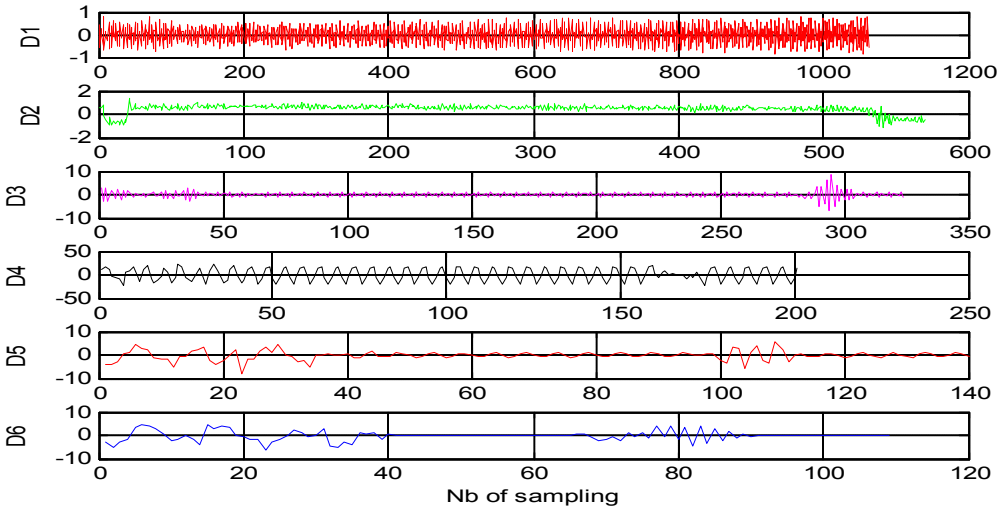

Fig. 8 – DWT of the stator current in case of unbalance fault.

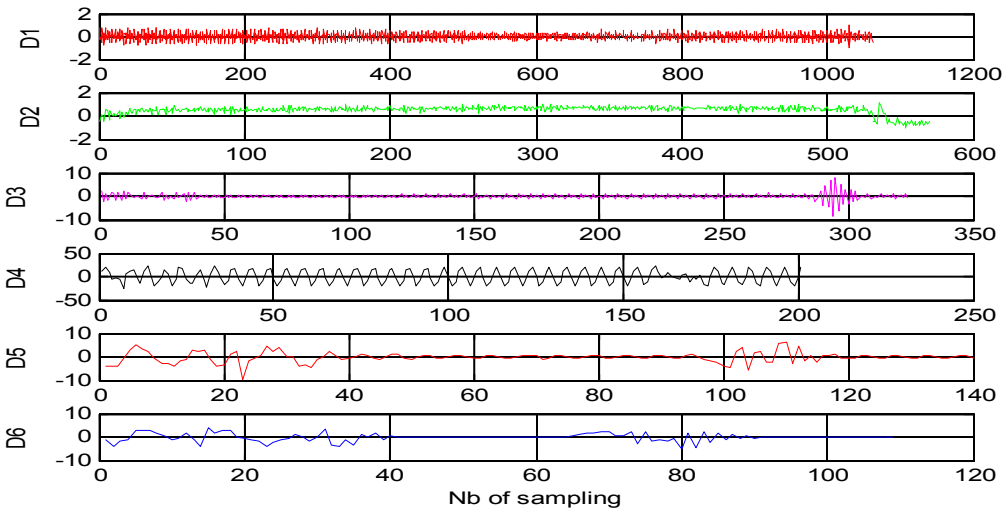

Fig. 9 – DWT of the stator current in case of misalignment fault.

3.4 Diagnosis using the relative energy

Figure 10 and its zoom in Figure 11 present the energy in each frequency band, a significant increase with respect to the healthy state appears in the energy of the higher level signals, especially for detail D4 where it is noted that there is a considerable deformation of the signal shape and a difference in amplitude with respect to the healthy signal. The oscillations of these signals are due to the presence of a mass unbalance default which was intentionally created by fixing a mass of 50 g on the shaft of the motor. The oscillations are consistent with the change in the characteristic frequency of the fault obtained by the Park vector FFT method. Therefore, it can be concluded that both methods indicate the presence of a mechanical fault at the system. And it can be observed that the energy stored in band 4 depends on the degree of the defect.

The calculation of the stored energy in each decomposition level in Figure 10 and Figure 11, confirms the increasing values observed in detail especially in level 4, which correspond to the band neighborhood and below of the fundamental.

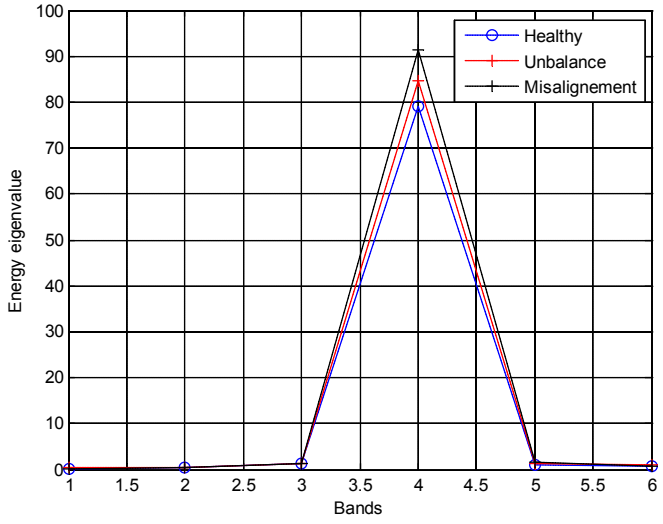

Fig. 10 – energy variation in the frequency bands (db44)

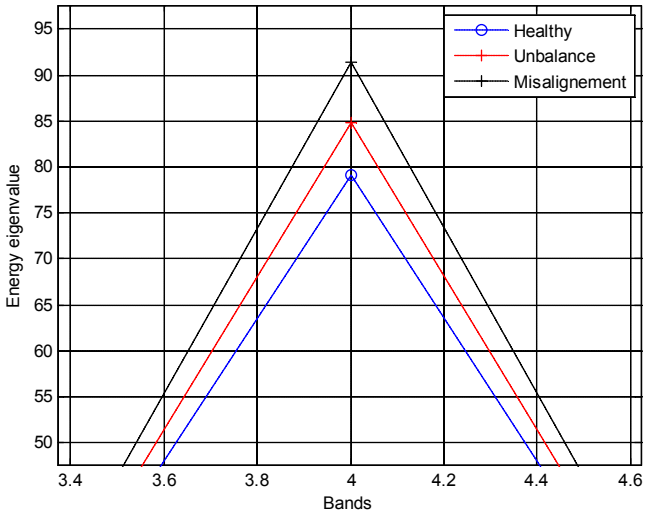

Fig. 11 – Zoom of the energy variation in frequency bands.

The energy corresponding to the level 4 in the healthy cases is 79.23%; however, it increases to 84.92% and 91.76% respectively in unbalance and misalignment fault. We can conclude that the difference between the healthy and the faulty cases is very clear, and the increase of energy differs according to fault severity level.

4 Conclusion

In this paper, the analysis of the current signature of the stator has contributed to the detection of mechanical faults such as unbalance and misalignment defects in an induction motor. Through this study, two methods of signal processing were presented: FFT and DWT. This dual approach has been theoretically presented and experimentally validated on a 2.6 kW three-phase industrial induction motor (Leroy Somer), in a healthy and degraded states.

Experimental results show that the wavelet transform approach (DWT) and the relative energy of the signal which is considered as a reliable criterion for comparing the healthy and degraded state of a system takes less response time than the FFT method. The wavelets have the advantage of being localized both in the time and frequency domain unlike the Fourier transform which is located only in the frequency domain. Feature extraction using fast Fourier transform (FFT) produces good results when the waveforms examined are stationary or periodic, but it is not suitable for non-stationary signals.

Admittedly, the DWT is a reliable and better technique than the FFT, but nevertheless, for the diagnosis and the predictive detection of the degradations affecting electrical machines, its role is much better as a complement to the FFT and not as its alternative.

The application of proposed methods associated with artificial intelligence approaches and other types of defects is currently under research.

REFERENCES

[1] Y. Merizalde, L. Hernández-Callejo and O. Duque-Perez, State of the art and trends in the monitoring, detection and diagnosis of failures in electric induction motors. Energies. Vol.10 (2017) pp. 1056.

[2] N. Bessous, S.E. Zouzou, W. Bentrah, S. Sbaa and M. Sahraoui, Diagnosis of bearing defects in induction motors using discrete wavelet transform. International Journal of Systems Assurance and Engineering Management. Vol.9 (2016), pp. 335-343.

[3] K.M. Siddiqui, K. Sahay, V.K. Giri, Early, diagnosis of bearing fault in the inverter driven induction motor by wavelet transform, In Proceedings of the IEEE International Conference on Circuit, Power and Computing Technologies (ICCPCT), Nagercoil, India, 18-19 March 2016, pp. 1-7.

[4] C. Verucchi, G. Bossio, J. Bossio, and G. Acosta, Fault detection in gear box with induction motors: an experimental study. IEEE Latin American Transactions , Vol.14 N°6 (2016) pp. 2726-2731

[5] G. Cablea, P. Granjon and C. Bérenguer, Three-phase electrical signals analysis for mechanical faults monitoring in rotating machine systems. Mechanical Systems and Signal Processing. Vol.92 (2017) pp. 278-292.
[6] D.H. Lee, J.H. Ahn and B.H. Koh, Fault detection of bearing systems through EEMD and optimization algorithm. Sensors. Vol.17 (2017) pp. 2477.
[7] G.K. Yamamoto, C. Da Costa and Da Silva Sousa, A smart experimental setup for vibration measurement and imbalance fault detection in rotating machinery. Case Studies in Mechanical Systems and Signal Processing, Vol.4 (2016) pp. 8-18.
[8] M. Agnes, Misalignment and shaft crack-related phase relationships for 1X and 2X vibration Components of Rotor Responses. Orbit, (1989) pp. 4-8.
[9] D. Goyal, B.S. Pabla, The vibration monitoring methods and signal processing techniques for structural health monitoring: a review. Archives of Computational Methods in Engineering. (2016) pp. 585-594.
[10] T. Mikhail, The Origin of the Electromagnetic Vibration of Induction Motors Operating in Modern Industry: Practical Experience - Analysis and Diagnostics. IEEE Transactions on Industry Applications, Vol.53 (2017) pp. 1669-1676.
[11] G. Suri, Loading effect on induction motor eccentricity diagnostics using vibration and motor current. Experimental Techniques, Rotating Machinery and Acoustics. Vol.8 (2015) pp. 273-280.
[12] M. Iorgulescu, R. Beloiu, Faults diagnosis for electrical machines based on analysis of motor current. In Proceedings of International Conference on Optimization of Electrical and Electronic Equipment (OPTIM), Bran, Romania, 22-24 May 2014. pp. 291–297.
[13] E.H. El-bouchikhi, V. Choqueuse, M. Benbouzid, Induction machine faults detection using stator current parametric spectral estimation. Mechanical Systems and Signal Processing. Vol.52-53(2015) pp. 447-464.
[14] H. Talhaoui, A. Menacer, A. Kessal, R.Kechida, Fast Fourier and discrete wavelet transforms applied to sensorless vector control induction motor for rotor bar faults diagnosis. ISA Trasactions. Vol.53 (2014) pp. 1639-1649.
[15] T. Ameid, A. Menacer, H. Talhaoui,I. Harzelli, Broken rotor bar fault diagnosis using fast Fourier transform applied to field-oriented control induction machine: simulation and experimental study. International Journal of Advanced Manufacturing and Technologies, Vol.92 (2017), pp. 917–928.
[16] I. Ouachtouk, S. Elhani, S. Guedira, K. Dahil , I. Sadiki, Advanced Model of Squirrel Cage Induction Machine for Broken Rotor Bars Fault Using Multi Indicators. Advances in Electrical and Electronic Engineering, Vol.14 (2016), pp. 512–521.
[17] J.R. Magdaleno, H.P. Barreto, J.R. Cortes, R.M. Caporal, I.C. Vega, Vibration Analysis of Partially Damaged Rotor Bar in Induction Motor under Different Load Condition Using DWT. Shock Vibration, Vol.1 (2016), pp. 1–12.
[18] A. Chaouch, M. Harir, A. Bendiabdellah, P. Remus, Instantaneous Power Spectrum Analysis To Detect Mixed Eccentricity Fault In Saturated Squirrel Cage Induction Motor, the 3rd international Conference on Automation , Control, Engineering and Computer Science, Tunisia, March 2016; p. 296–300.
[19] W. Wroński W., M. Sułowicz, A. Dziechciarz, Dynamic and Static Eccentricity Detection in Induction Motors in Transient States. Technical Transactions Electrical Engineering, Vol.112 (2015), pp. 171–194.
[20] J. Faiz, S.M.M. Moosavi, Detection of mixed eccentricity fault in doubly-fed induction generator based on reactive power spectrum. IET Electric Power Applications, Vol. 11(2017), pp. 1076–1084.
[21] N. Bessous, S.E. Zouzou,W. Bentrah, S Sbaa, A comparative study between the MCSA, DWT and the vibration analysis methods to diagnose the dynamic eccentricity fault in induction motors. The 6th International Conference on Systems and Control (ICSC), Batna, Algeria, 7–9 May 2017; pp. 414–421.
[22] C. Verucchi, J. Bossio, G. Bossio, G. Acosta, Misalignment detection in induction motors with flexible coupling by means of estimated torque analysis and MCSA. Mechanical Systems and Signal Processing, Vol.80 (2016), pp. 570–581.
[23] W.T. Thomson, R.J. Gilmore, Motor Current Signature Analysis to Detect Faults in Induction Motor Drives-Fundamentals, Data Interpretation, and Industrial Case Histories. In Proceedings of the Thirty-Second Turbomachinery Symposium, Houston, Texas, USA, 8–11 September 2003; pp. 145–156.
[24] Z. Jafar, P. Javed, An Advanced Park's Vectors Approach for Bearing Fault Detection. Tribology Interantional **,** Vol.42 (2009), pp. 213–219.
[25] N. Mehla, R. Dahiya, Detection of Bearing Faults of Induction Motor Using Park's Vector Approach. International Journal of Engineering and Technology, Vol.2 (2010), pp. 263–266.
[26] J.O. Estima, N.M.A. Freire, A.J.M. Cardoso, Recent advances in fault diagnosis by Park's vector approach. In the IEEE Workshop on Electrical Machines Design Control and Diagnosis (WEMDCD), Paris, France, 11–12 March 2013, pp. 279–288.

[27] S.H. Lee, K. Sungshin, J.M. Kim, M.H. Lee, Fourier and wavelet transformations for the fault detection of induction motor with stator current. In the 30th Annual Conference of IEEE Industrial Electronics Society (IECON), Korea, 2–6 November 2004; pp. 383-388.

[28] N. Bessous, S.E. Zouzou , W. Bentrah , S. Sbaa , A Comparative Study between the FFT and DWT Method Applied to a Bearing Fault in Induction Motors – Results Dedicated to the Industry. WSEAS Transactions on Systems and Control, Vol. 10 (2015), pp. 616–623.

[29] T.W.S. Chow, S. Hai, Induction machine fault diagnostic analysis with wavelet technique. IEEE Transactions on Industrial Electronics, Vol.51 (2004), pp 558–565.

[30] M. Nasir Uddin , M. Mizanur Rahman , Online current and vibration signal monitoring based fault detection of bowed rotor induction motor. In Proceedings of the IEEE Energy Conversion Congress and Exposition (ECCE), Montreal, QC, Canada, 20–24 September 2015; p. 2988–2994.

[31] M. Mizanur Rahman, M. Nasir Uddin , Online Unbalanced Rotor Fault Detection of an IM Drive Based on Both Time and Frequency Domain Analyses. IEEE Transsactions on Industrial Appl**,** Vol.53 (2017), pp. 4087–4096.

[32] B. Alain, C. Pachaud, « Aide-mémoire , Surveillance des machines par analyse des vibrations » Paris, Dunod, 2009 ISBN 978-2-10-054190-4

[33] M.R. Mehrjou, N.M. Mariun, M. Karami, S.B.Mohd Noor, N. Mirson, M.Z.A. Ab Kadir, A. Mohd Radzi Mohd, M.H. Marhaban, Wavelet-Based Analysis of MCSA for Fault Detection in Electrical Machine. In Wavelet Transform and Some of Its Real-World Applications, 1st ed.; Baleanu, D.; InTech, 2015; Chapter 5, pp. 79–110

[34] H. Cherif, A. Menace, B. Bessam, R. Kechida , Stator Inter Turns Fault Detection Using Discrete Wavelet Transform. In Proceedings of the 10th IEEE International Symposium on Diagnostics for Electrical Machines, Power Electronics and Drives (SDEMPED), Guarda, Portugal, 1–4 September 2015; p.138–142.

[35] I. Daubechies, The wavelet transform, time-frequency localization and signal analysis. IEEE Trans Inf Theory, Vol.36 (1990), pp. 961–1005.

[36] Z.K. Peng, F.L. Chu, 2004. Application of the wavelet transform in machine condition monitoring and fault diagnostics: a review with bibliography. Mechanical Systems and Signal Processing, 18, p. 199–221.